doi:10.1038/nature11179

Introduction

The DNA damage response (DDR) is a coordinate set of events that promptly follows the generation of a lesion in the DNA double helix. Detection of DNA discontinuities by specialized factors initiates a signaling cascade that, stemming from the site of DNA damage, amplifies the signal and reaches the whole nuclear space and the entire cell[3]. Detection of a DSB triggers the activity of the protein kinase ATM that, among other factors, phosphorylates the histone variant H2AX (phosphorylated H2AX or γH2AX) at the DNA damage site. This modification recruits DDR-mediators like MDC1 and 53BP1 that boost ATM activity. DDR activation can be triggered by exogenous DNA damaging agents such as ionizing radiations and by endogenous physiological events such as meiotic recombination and telomere shortening, as well as pathological events such as oncogene activation or viral infections[3]. Telomeres dysfunction and oncogene activation can generate a sustained DDR leading to a permanent cell-cycle arrest known as cellular senescence[11].

It has recently been observed that a significant fraction of transcripts in a cell do not encode for proteins[4]. These non-coding RNAs (ncRNAs) play a variety of nuclear functions. Some may remain associated with chromatin, and some aggregate in subnuclear structures such as speckles and paraspeckles[5]. An unsuspected increasing number of these ncRNA transcripts have been shown to be evolutionarily conserved among related species[31,32] and play a role in relevant cellular functions by regulating the localization and the activity of proteins or providing structural support for cellular and sub-cellular structures[33], controlling chromatin-modification[34,5] and acting as enhancers[35]. Some ncRNAs are processed by ribonucleases of the RNA interference (RNAi) pathway, giving rise to small double-stranded RNA products that participate

in various cellular functions. The RNAi pathway is an evolutionary conserved machinery, whose components are thought to have evolved to preserve genome integrity from the attacks of viruses and mobile genetic elements[36]. It involves different types of small double-stranded RNA molecules including small interfering RNAs (siRNAs), microRNAs, repeat-associated small interfering RNAs (rasiRNAs), Piwi-interacting RNAs (piRNAs)[37] and QDE-2 interacting RNAs (qiRNA) in Neurospora crassa[38]. RNAi is commonly thought to act by two posttranscriptional mechanisms: translational repression and mRNA decay. GW182-like proteins, TNRC6A, B and C in mammals are essential mediators of RNAi, they repress translation and promote mRNA degradation[39,15]. MicroRNAs-dependent gene expression regulation have been involved in several processes such as cell fate determination, transformation, proliferation and cell death[40]. piRNAs and qiRNAs have been implicated in genome stability maintenance[38] and a family of microRNAs (miR-34) has been shown to act downstream of p53[41]. It is unknown whether small RNAs have any direct role in the control of DDR activation at sites of DNA damage.

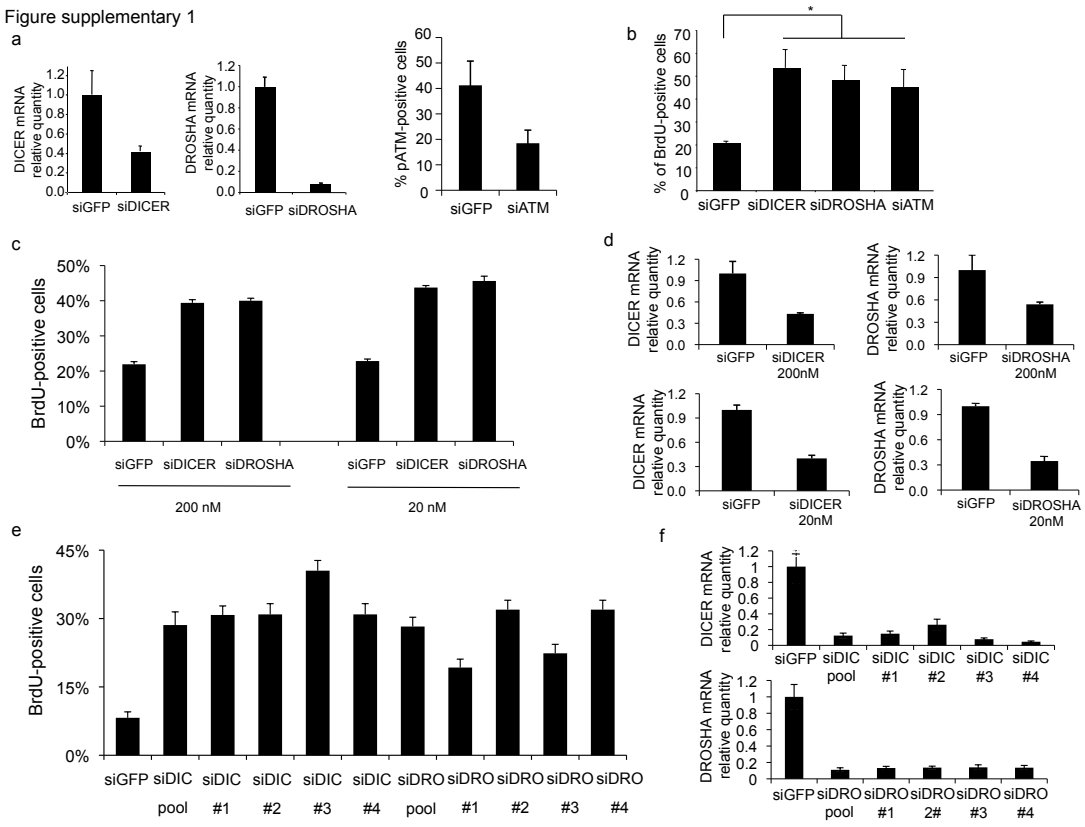

Figure Supplementary 1| siRNA against DICER or DROSHA in pools at different concentrations and individually reproducibly allow escape of OIS cells from senescence. a. DICER or DROSHA knockdown by siRNA pools in OIS cells were evaluated by qRT-PCR. ATM knockdown by siRNA pool was evaluated by immunofluorescence and quantified as percentage of cells positive for pATM staining. **b.** DICER or DROSHA knockdown in OIS cells by siRNA increases BrdU incorporation rates. Histogram shows the percentage of BrdU-positive cells. siGFP was used as control. Error bars indicate s.e.m. (n ≥ 3). Differences are statistically significant (*p-value < 0.001). **c.** Different concentrations (10 fold difference) of siRNA pools against DICER or DROSHA in OIS cells allow escape from senescence. Error bars indicate s.e.m. For the quantification shown more then 100 cells were analysed. **d.** Knockdown was evaluated by qRT-PCR. **e.** siRNA pools against DICER or DROSHA used in OIS cells were deconvolved and siRNAs were individually tested and reproducibly allowed escape from senescence. Error bars indicate s.e.m. For the quantification shown more then 300 cells were analysed. **f.** Knockdown was evaluated by qRT-PCR.

Figure supplementary 2

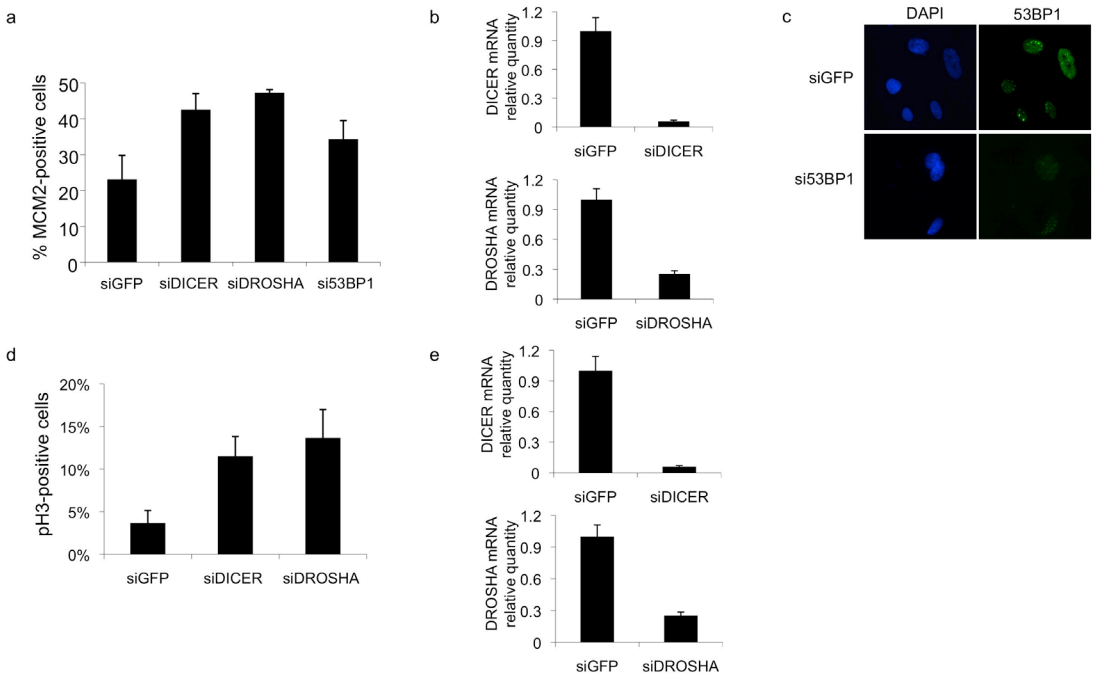

Figure Supplementary 2| DICER or DROSHA inactivation in OIS cells allows cell-cycle progression. a. DICER-, DROSHA- and 53BP1-inactivation by transfection with siRNA pools in OIS cells induces MCM2 expression, a marker of chromosomal DNA replication. Error bars indicate s.e.m. For the quantification shown more then 100 cells were analysed. **b.** DICER and DROSHA knockdown was evaluated by qRT-PCR. **c.** 53BP1 knockdown was evaluated by immunofluorescence. **d.** DICER- and DROSHA-inactivated OIS cells re-express pH3, a marker of entry into mitosis. Error bars indicate s.e.m. For the quantification shown more then 100 cells were analysed. **e.** DICER and DROSHA knockdown was evaluated by qRT-PCR.

Figure supplementary 3

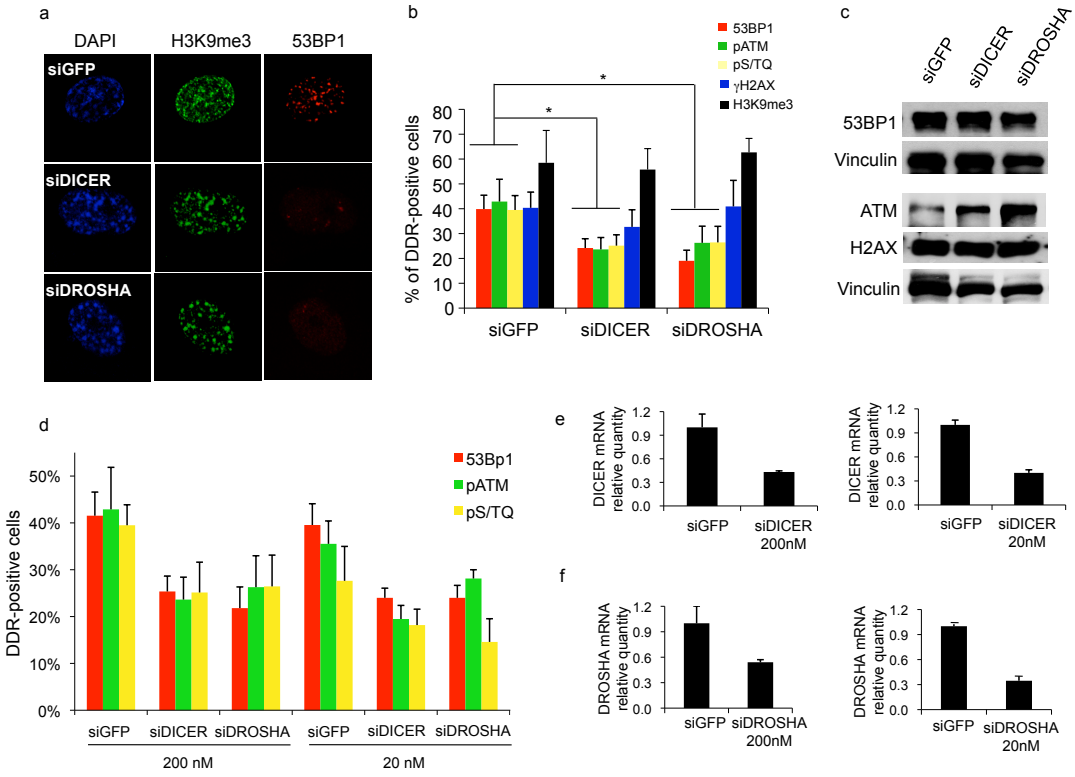

Figure Supplementary 3| DICER or DROSHA knockdown in OIS cells does not decrease SAHF or DDR protein levels but impairs DDR activation. a. DICER or DROSHA were knockdown by siRNA. Cells were stained for H3K9me3 SAHF marker and for 53BP1. siGFP was used as control. DICER or DROSHA inactivation affects 53BP1 foci without altering SAHF stability. **b**. Histograms show the percentage of cells positive for 53BP1, pATM, pS/TQ and γH2AX or SAHFs as detected by H3K9me3. Error bars indicate s.e.m. (n ≥ 3). Differences are statistically significant (*p-value < 0.05). **c**. Immunoblot analysis of 53BP1, ATM and H2AX in DICER- or DROSHA- inactivated OIS cells. Vinculin is used as loading control. **d**. Different concentrations (10 fold difference) of siRNA pools against DICER or DROSHA in OIS cells impair DDR foci detection. Error bars indicate s.e.m. For the quantification shown around 100 cells were analysed. **e, f**. Knockdown was evaluated by qRT-PCR.

Figure supplementary 4

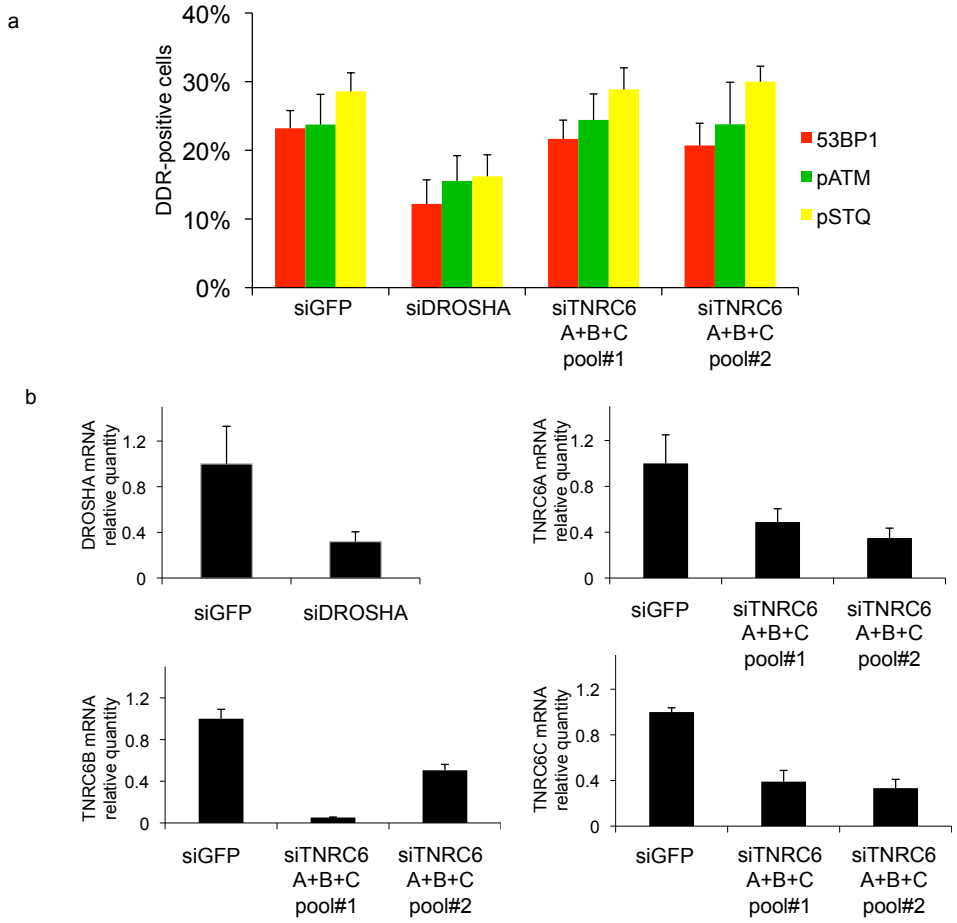

Figure Supplementary 4| Simultaneous inactivation of TNRC6A, B and TNC6C in OIS cells does not affect DDR foci formation, while DROSHA inactivation does. a. OIS cells inactivated by siRNA for DROSHA or TNRC6A, B and C simultaneously (with two independent pools of siRNAs: pool #1 and #2) were stained for 53BP1, pATM and pS/TQ. TNRC6A, B and C concomitant inactivation with either siRNA pools #1 or #2 has no detectable effect on DDR. Error bars indicate s.e.m. For the quantification shown more than 100 cells were analysed. **b.** Knockdown was evaluated by qRT-PCR.

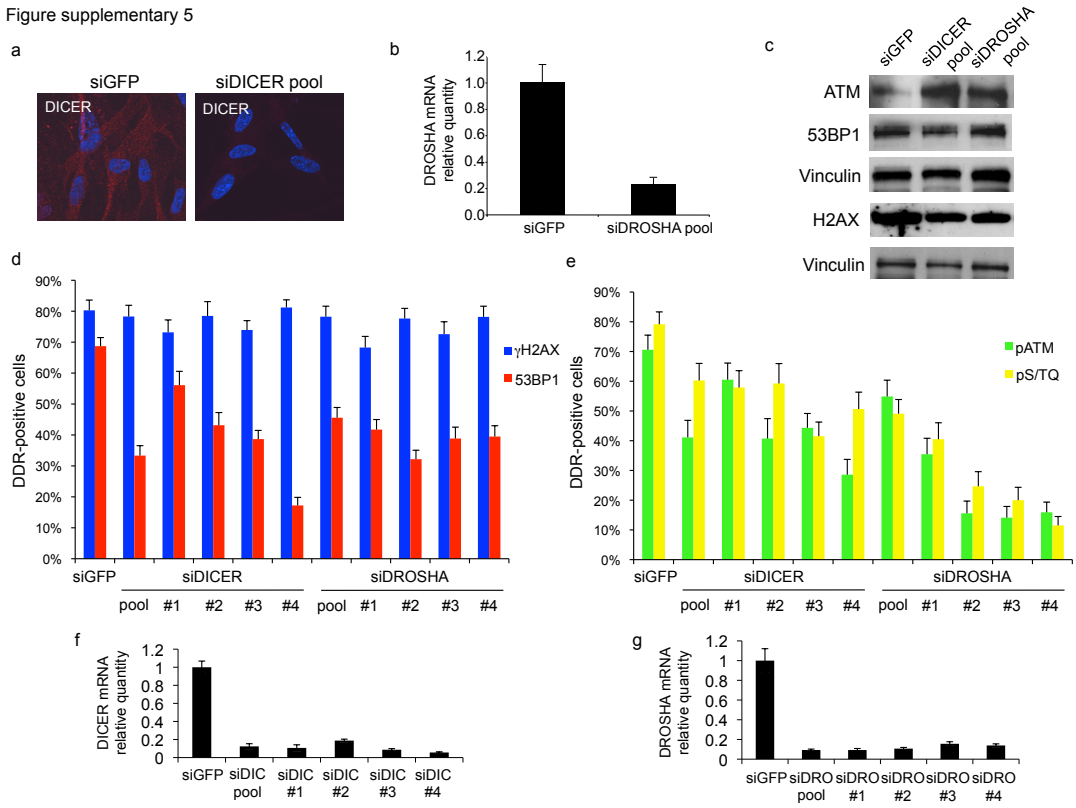

Figure Supplementary 5| DICER or DROSHA inactivation in HNF impairs IR-induced DDR foci formation. a, b. Efficiency of DICER or DROSHA knockdown in WI38 human fibroblasts was evaluated by immunostaining (**a**) and qRT-PCR (**b**), respectively. **c.** Immunoblot analysis of ATM, 53BP1 and H2AX proteins expression levels in DICER- or DROSHA-inactivated WI38. siGFP transfected cells are used as control. Vinculin is used as loading control. **d, e**. siRNA pools against DICER or DROSHA were deconvolved and siRNAs were used individually. They all reduce DDR (53BP1, pATM and pS/TQ, but not γH2AX) foci formation. Error bars indicate s.e.m.. For the quantification shown around 100 cells from two independent experiments were analysed. **f, g** Knockdown was evaluated by qRT-PCR.

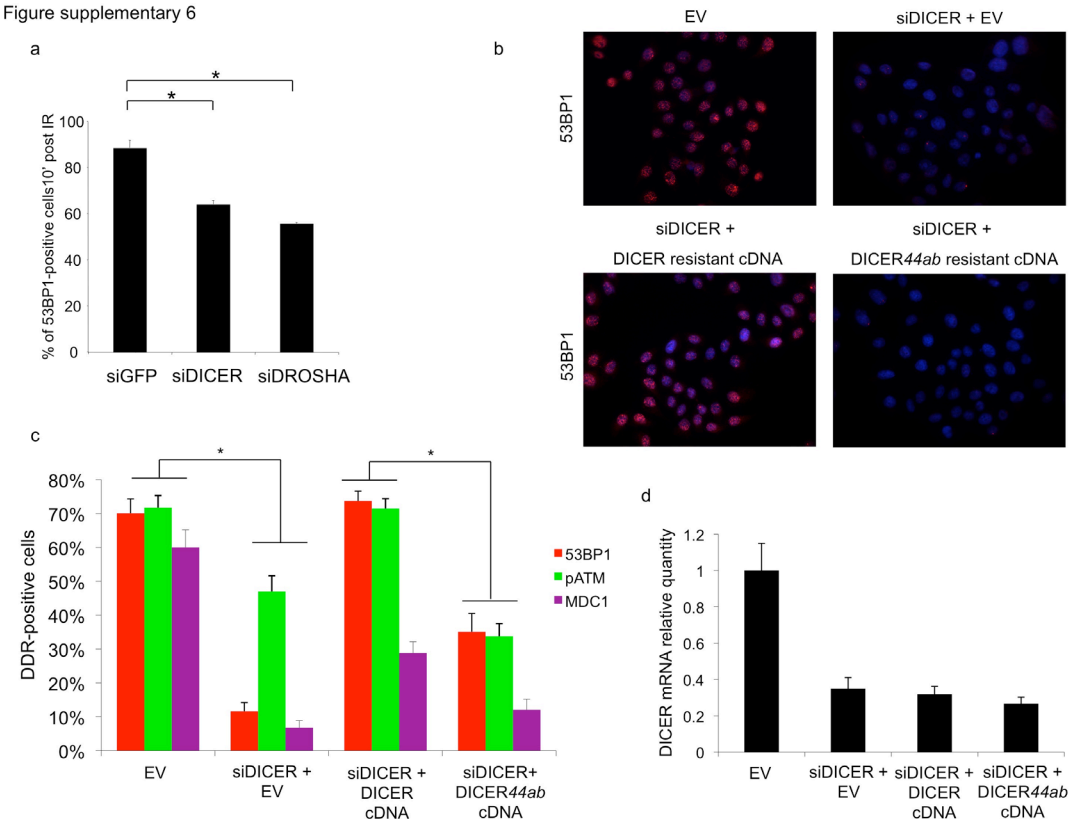

Figure Supplementary 6| 53BP1 foci formation is delayed upon DICER or DROSHA knockdown and impaired 53BP1 foci formation is rescued by wild-type but not mutant DICER. a. 53BP1-foci formation is impaired 10 minutes post IR (5 Gy) in WI38 cells knocked-down for DICER or DROSHA by siRNA pools. Histogram shows the percentage of cells positive for 53BP1 foci. Differences are statistically significant (*p-value< 0.05). (n=3). **b**. Expression of siRNA-resistant WT DICER, but not of the mutant allele DICER44ab lacking endonuclease activity, rescues DDR foci formation defect in DICER knocked-down HeLa cells. 53BP1 foci formation was studied 10' after IR (2 Gy), pATM and MDC1 1 hour afterward. **c.** Histogram shows the percentage of cells positive for DDR foci. Error bars indicate s.e.m. For the quantification shown around 100 cells were analysed. **d.** Knockdown of endogenous DICER by 3'UTR siRNA was evaluated by qRT-PCR.

Figure supplementary 7

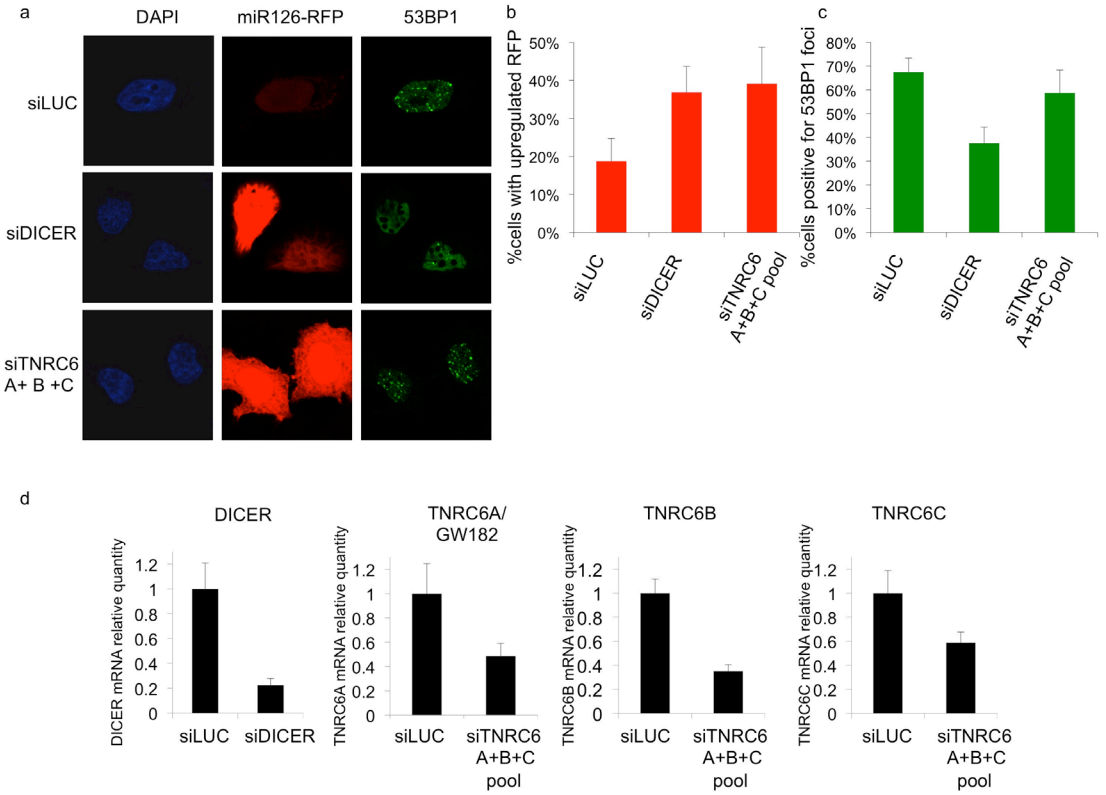

Figure Supplementary 7| DICER inactivation or TNRC6 A, B and C, simultaneous inactivation in HeLa cells is associated with similar up-regulation of RFP-miR126 reporter signal but DDR foci are impaired only in DICER-inactivated cells a. HeLa cells were transfected with a reporter vector carrying three binding sites for miR-126 in the 3'UTR of the RFP mRNA together with siRNAs pools against DICER or TNRC6A, B and C. Cells were irradiated (2Gy) and stained for 53BP1 10' later. **b.** Both DICER and GW182-like proteins inactivation resulted in the upregulation of the miR126-sensitive RFP reporter but (**c**) only DICER inactivation affects DDR activation. For the quantification shown around 50 cells were analysed. Error bars indicate s.e.m. **d**. Knockdown was evaluated by qRT-PCR.

Figure supplementary 8

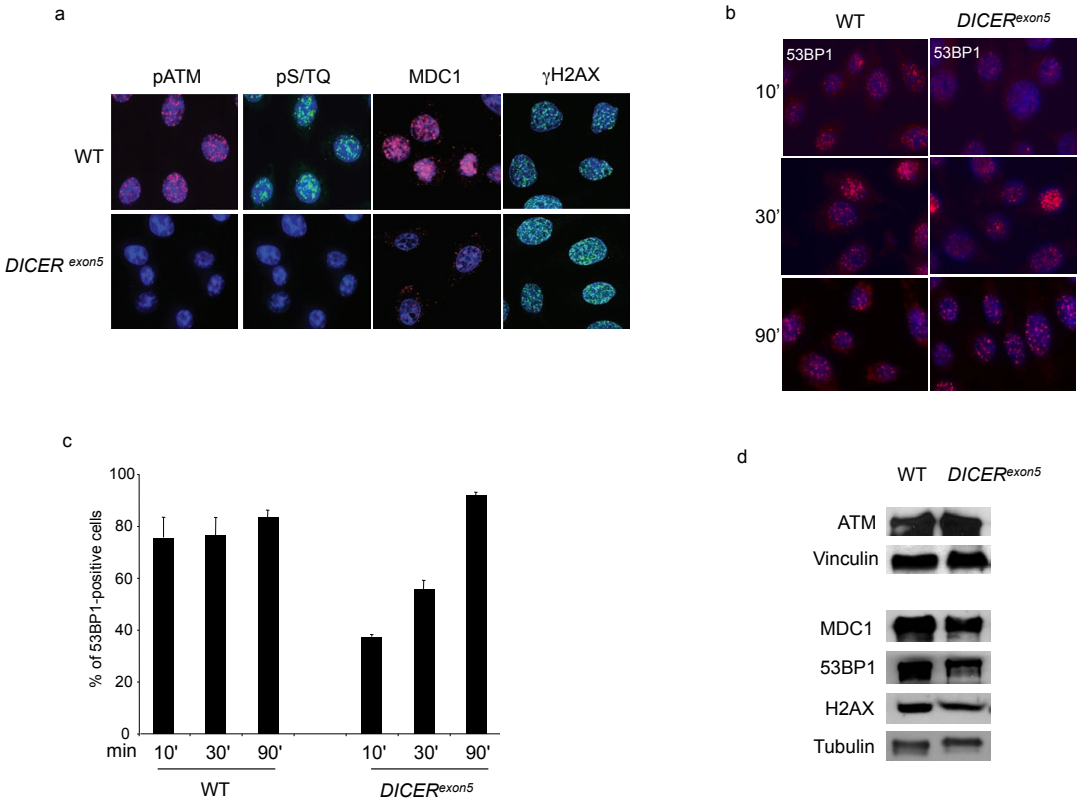

Figure Supplementary 8| pATM, pS/TQ and MDC1 foci are impaired and 53BP1 foci formation is delayed in *DICER*^{exon5} cells despite normal DDR factors expression. a. WT and *DICER*^{exon5} cells were irradiated (2Gy) and fixed 2h later. pATM, pS/TQ and MDC1, but not γH2AX, foci formation is impaired in *DICER*^{exon5}cells. **b**. Irradiated *DICER*^{exon5} cells have delayed 53BP1-foci formation. Images show 53BP1-foci at 10, 30 and 90 minutes post IR (2 Gy) in wild-type (WT) and *DICER*^{exon5} cells. **c.** Histograms show the percentage of cells positive for 53BP1 foci. Error bars indicate s.e.m. For the quantification shown around 200 cells from two independent experiments were analysed. **d**. Immunoblot analysis of ATM, MDC1, 53BP1 and H2AX in wild-type (WT) and *DICER*^{exon5} cells. Vinculin and Tubulin are used as loading control.

Figure supplementary 9

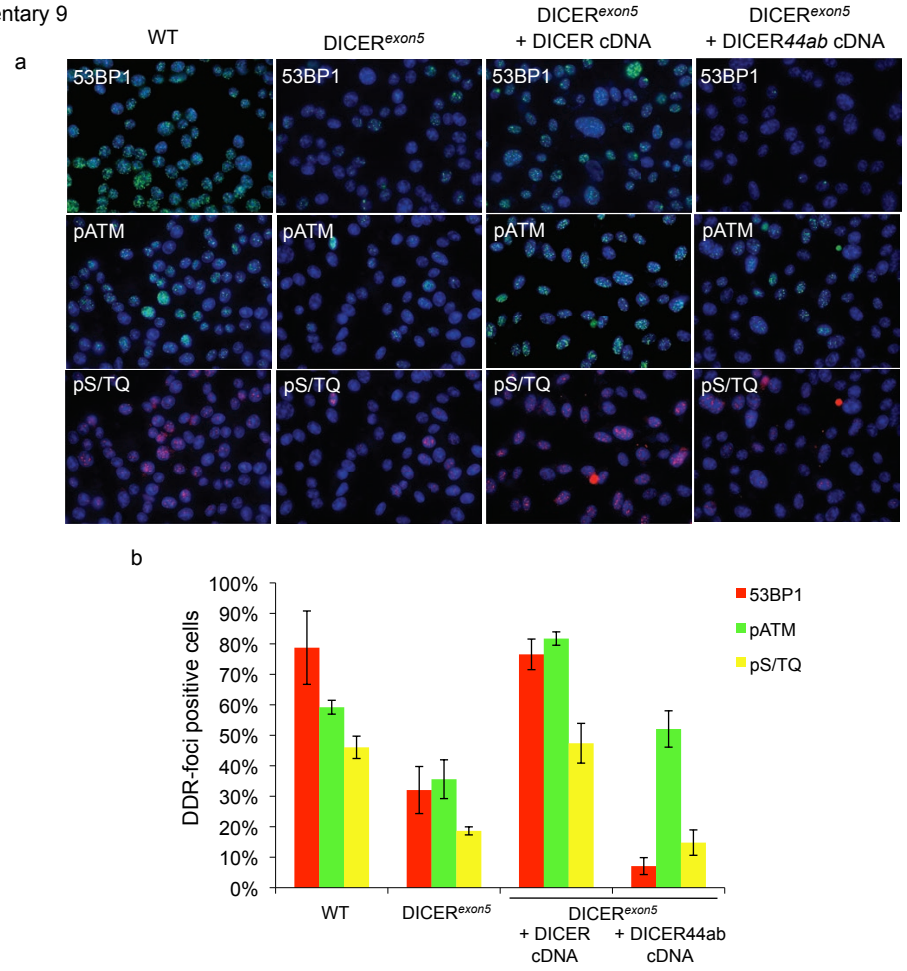

Figure Supplementary 9| Impaired DDR foci formation in *DICER*^{exon5} cells is rescued by wild-type but not mutant DICER. a. Expression of WT DICER but not the mutant allele DICER44ab, restores DDR foci formation defects in *DICER*^{exon5} cells. 53BP1 foci formation was studied 10' after IR (2 Gy), pATM and pS/TQ 1 hour afterward. **b**. Histograms show the percentage of cells positive for the indicated DDR foci. Error bars indicate s.e.m. For the quantification shown around 200 cells were analysed.

Figure supplementary 10

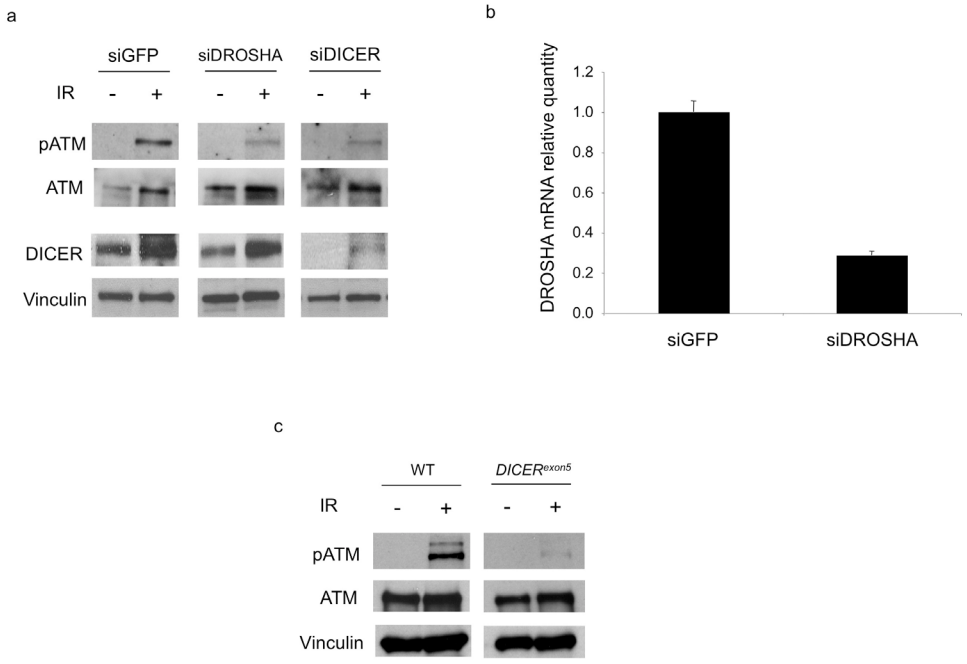

Figure Supplementary 10| ATM activation as detected by autophosphorylation is impaired in DICER- and DROSHA-inactivated cells. a. ATM activation following IR (10 Gy) is impaired in DICER or DROSHA knocked-down WI38 human fibroblasts as detected by immunoblot analysis for pATM. siGFP transfected cells are used as a positive control for ATM activation. Total ATM is not reduced. DICER knockdown was evaluated by immunoblot analysis**. b.** DROSHA knockdown in WI38 cells was evaluated by qRT-PCR. **c**. ATM activation is impaired in irradiated (2 Gy) *DICER*^{exon5} cells**.** Total ATM and Vinculin are used as loading control.

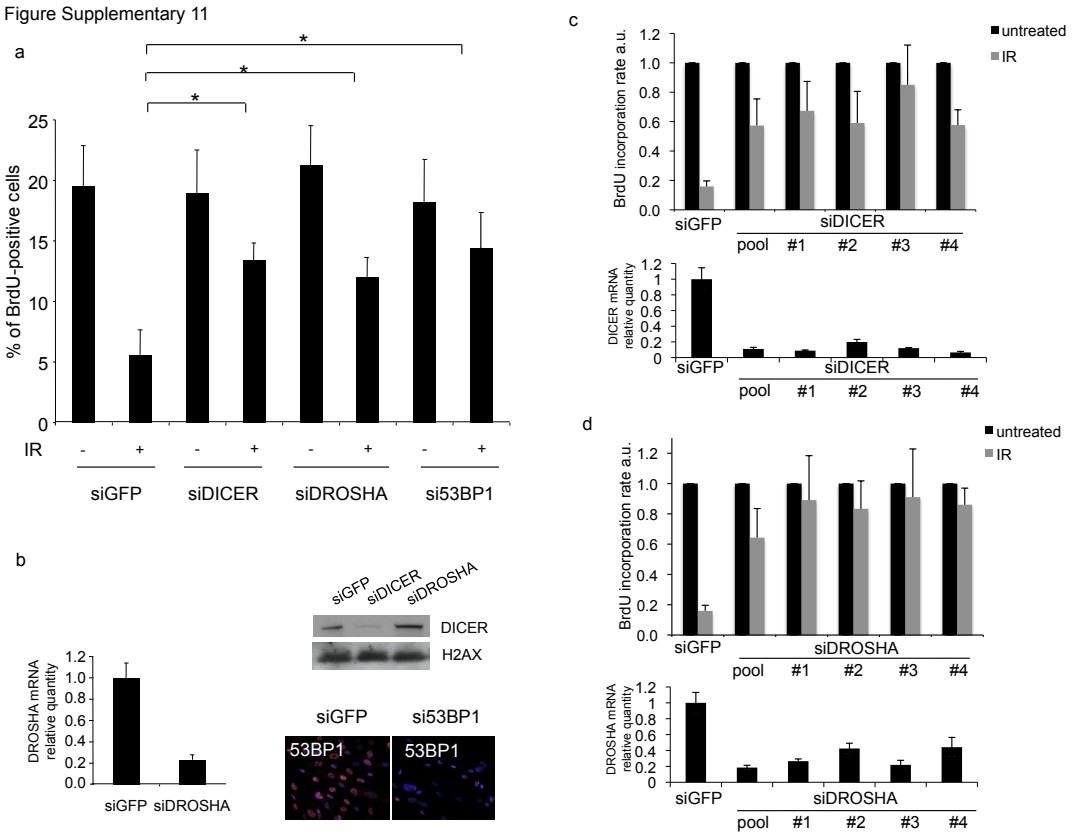

Figure Supplementary 11| DICER or DROSHA knockdown impairs G1/S checkpoint. a. DICER, DROSHA or 53BP1 knockdown by siRNA pools in WI38 impairs irradiation-induced G1/S checkpoint. siGFP was used as control. Cells were irradiated (10Gy) and labeled with BrdU for 7 hours before fixation. Histograms show the percentage of BrdU-positive cells in not-irradiated (-) and in irradiated (+) cells. Error bars indicate s.e.m. (n=3). Differences are statistically significant (**p-value*<0.05). **b.** DICER, DROSHA and 53BP1 knockdowns by siRNA pools in WI38 cells were monitored by qRT-PCR, immunoblot and immunofluorescence, respectively. DICER **(c)** and DROSHA **(d)** siRNA pools were deconvolved and siRNAs were used individually and they reproducibly impaired G1/S checkpoint activation in WI38 cells. Histogram shows the percentage of BrdU positive cells before (black bar) and after IR (gray bar) upon normalization on the percentage of BrdU-positive cells before IR for each cell line. For the quantification shown more than 100 cells were analysed. Error bars indicate s.e.m. Knockdown was evaluated by qRT-PCR.

Figure supplementary 12

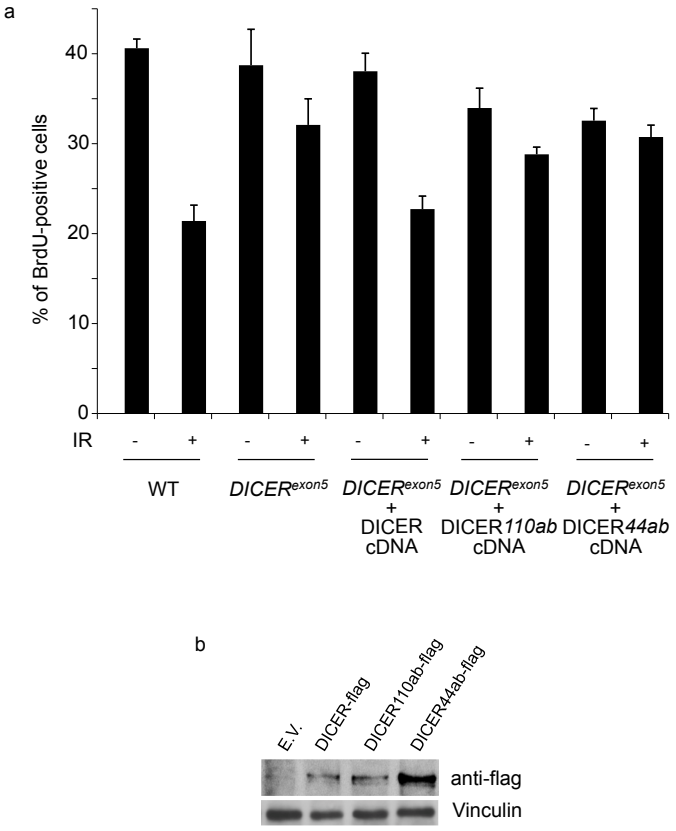

Figure Supplementary 12| Loss of G1/S checkpoint activation in *DICER*^{exon5} cells is restored by wild-type DICER cDNA re-expression but not by DICER mutant alleles. a. DICER-flag cDNA transfection into *DICER*^{exon5} cells restores a proficient G1/S checkpoint post IR (2 Gy). DICER110ab-flag and DICER44ab-flag double mutants carry two amino acid substitution in the RNase III domains of DICER and are both defective in endonuclease activity. Histograms show the percentage of BrdU-positive cells. Error bars indicate s.e.m. For the quantification shown more than 500 cells were analysed. **b**. Immunoblot analysis against flag-epitope shows the expression of DICER alleles.

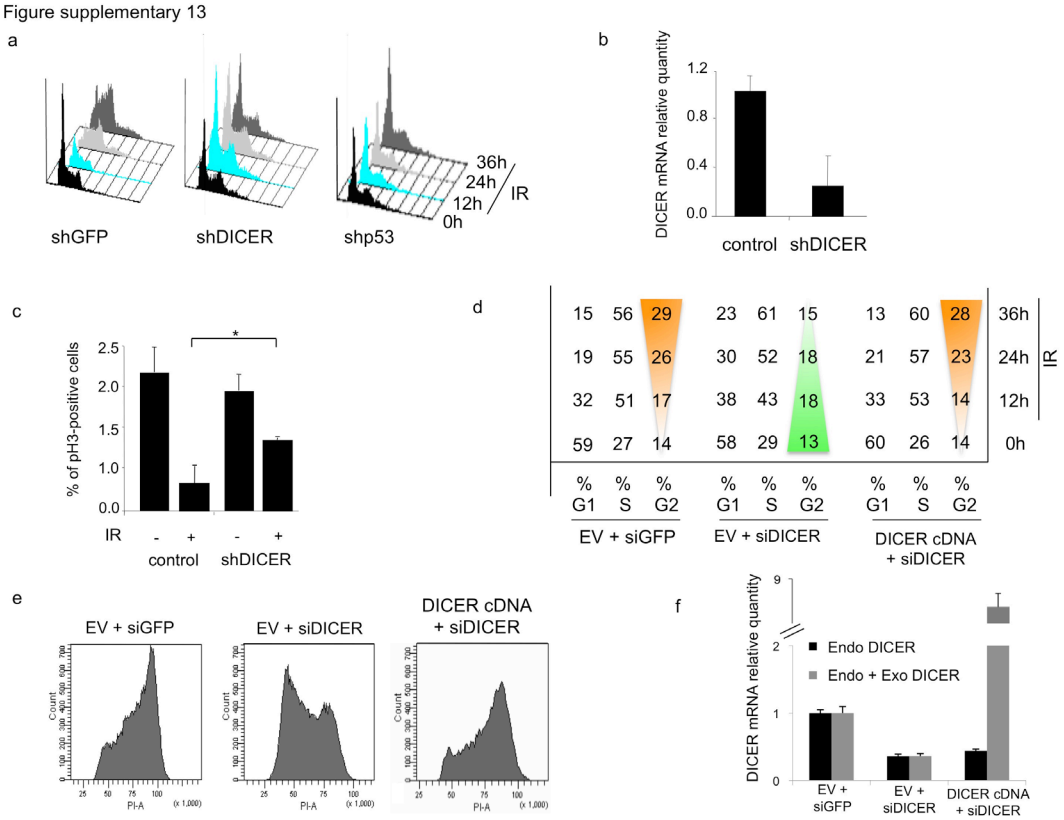

Figure Supplementary 13| Loss of G2/M checkpoint activation in DICER-inactivated cells. a. DICER knocked-down cells have impaired G2/M checkpoint**.** FACS profiles of HEK293 cells transfected with an shRNA against DICER or against p53 at 12, 24 and 36 hours post irradiation (5Gy). shGFP is used as control. **b**. DICER knockdown by shRNA in HEK293 cells was monitored by qRT-PCR. **c**. DICER-inactivated HEK293 cells have impaired G2/M checkpoint as detected by pH3 immunostaining of mitotic cells in not irradiated (-) and 24h post IR (+). Histograms show the percentage of pH3 positive cells in control and DICER-inactivated cells. Error bars indicate s.d. (n=3). Differences are statistically significant (*p-*value*<0.05). **d.** DICER knocked-down cells have an impaired G2/M checkpoint that can be restored upon transfection of siRNA-resistant DICER. The table shows the percentage of cells in G1, S and G2 phase of the cell cycle at different time points post IR. **e.** FACS profiles of HEK293 cells transfected with the indicated combinations of siRNA and vectors (EV stands for empty vector), 36 hours post IR (5Gy). **f**. Endogenous DICER (Endo DICER) knockdown and exogenous DICER (Exo DICER) overexpression were evaluated by qRT-PCR.

Figure Supplementary 14

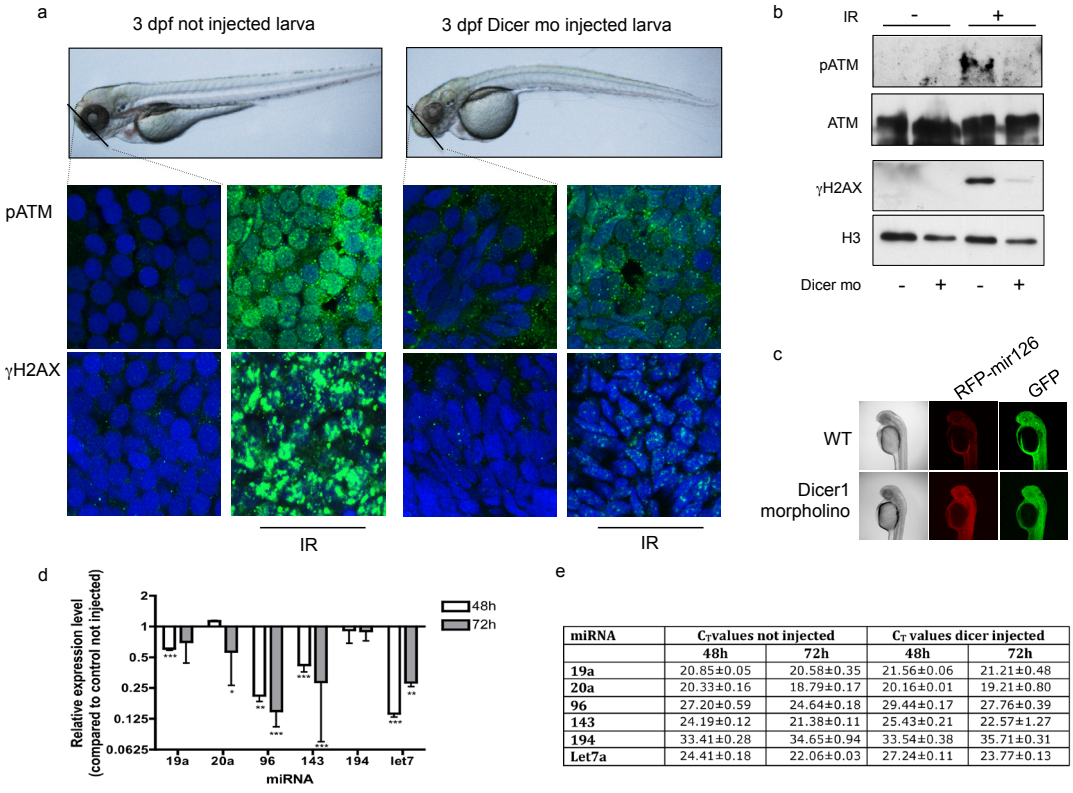

miRNA	$C_T$values not injected		C_T values dicer injected	
	48h	72h	48h	72h
19a	20.85±0.05	20.58±0.35	21.56±0.06	21.21±0.48
20a	20.33±0.16	18.79±0.17	20.16±0.01	19.21±0.80
96	27.20±0.59	24.64±0.18	29.44±0.17	27.76±0.39
143	24.19±0.12	21.38±0.11	25.43±0.21	22.57±1.27
194	33.41±0.28	34.65±0.94	33.54±0.38	35.71±0.31
Let7a	24.41±0.18	22.06±0.03	27.24±0.11	23.77±0.13

Figure Supplementary 14| Dicer1 morpholino-injected zebrafish embryos display a defect in pATM and γH2AX accumulation post IR. a. 3 days post fertilization (dpf) larvae injected with RFP-miR126 sensor mRNA alone or with Dicer1 morpholino. Note the jaw defects and small eye indicative of developmental delays in the Dicer1 morpholino-injected embryos. Images illustrate the location of the sections from the head of WT (not injected) and Dicer1-morpholino injected zebrafish larvae stained for pATM and γH2AX before and after irradiation (12 Gy). Sections were stained with DAPI and pATM or γH2AX antibody. The increased sensitivity of H2AX phosphorylation to Dicer1 inactivation in zebrafish compared to mammals is likely due to the apparent lack of the catalytic subunit of DNAPK in the zebrafish genome (unpublished observation), which makes any impact on ATM kinase activity more noticeable in terms of H2AX phosphorylation. **b**. Immunoblot analysis of pATM and γH2AX accumulation in extracts from not irradiated and irradiated wild-type embryos or Dicer1 morpholino-injected embryos. Total ATM and histone H3 were used as loading control. **c**. Specificity of miR126 sensor. Images show the expression levels of RFP-miR126 sensor and GFP in uninjected and Dicer1 morpholino injected larvae. Dicer inactivation results in the specific up-regulation of RFP-miR126 sensor, while GFP is unchanged. **d**. miRNAs expression of 48 and 72 hours post fertilization larvae injected or not with Dicer1 morpholino were analyzed by real-time PCR. Data are expressed as relative expression level in Dicer1 morpholino-injected embryos compared to the control embryos and are the mean of two independent pools of embryos performed in duplicate. **e.** Table of raw C_T values.

Figure supplementary 15

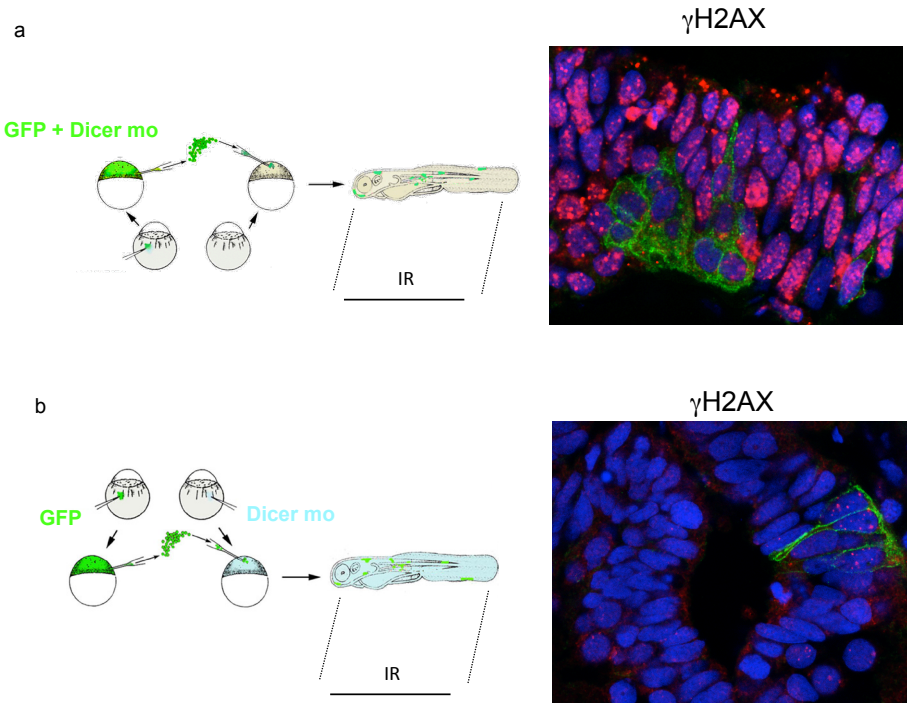

Figure Supplementary 15| Irradiation-induced γH2AX accumulation is impaired in Dicer1 morpholino-injected cells in chimaeric animals. a. Schematic drawing of the transplantation procedure: cells from embryos injected with Dicer1 morpholino and mRNA encoding for GFP were transplanted at blastula stage into control embryos. Chimaeric larvae were irradiated at 3 days post fertilization (dpf) and stained with antibodies against γH2AX. GFP-positive Dicer1 morpholino transplanted cells, integrated in various locations in the host, show reduced γH2AX signals following IR. **b**. Schematic drawing of the reverse transplantation procedure: control cells from embryos injected with mRNA encoding for GFP were transplanted into Dicer1 morpholino injected embryos. Chimaeric larvae were irradiated as above and stained with antibodies against γH2AX. Dicer1-expressing cells display γH2AX signals, while the surrounding Dicer1 morpholino-injected cells do not.

Figure supplementary 16

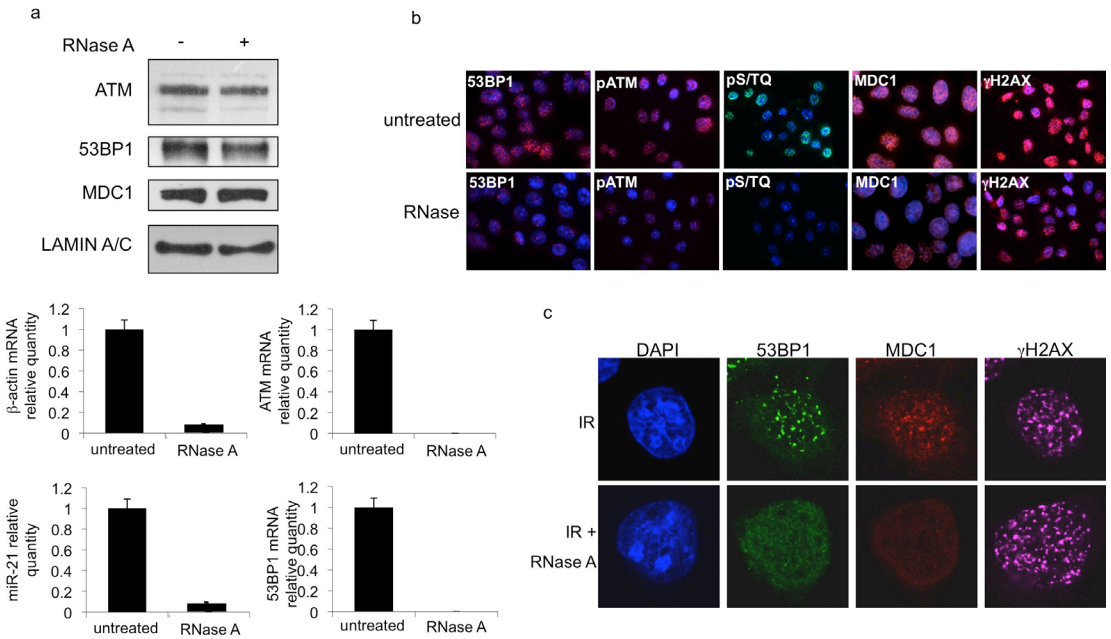

Figure Supplementary 16| RNase A treatment degrades both mRNAs and microRNAs and compromises DDR activation without altering DDR protein levels. a. RNase A treatment does not affect DDR proteins (ATM, 53BP1, MDC1) stability. Lamin A/C is used as loading control. qRT-PCR analysis of β-actin, 53BP1 and ATM mRNA and miR-21, in mock and RNase A-treated cells. Error bars indicate s.d. (n=3). Differences are statistically significant (p-value<0.05). **b.** Irradiated (2 Gy) HeLa cells were treated with PBS (-) or RNase A and probed for 53BP1, pATM, pS/TQ, MDC1 and γH2AX foci. 53BP1, pATM, pS/TQ and MDC1, but not γH2AX, foci are strongly reduced upon RNase A treatment. **c.** RNase A affects 53BP1 and MDC1 but not γH2AX at individual foci.

Figure supplementary 17

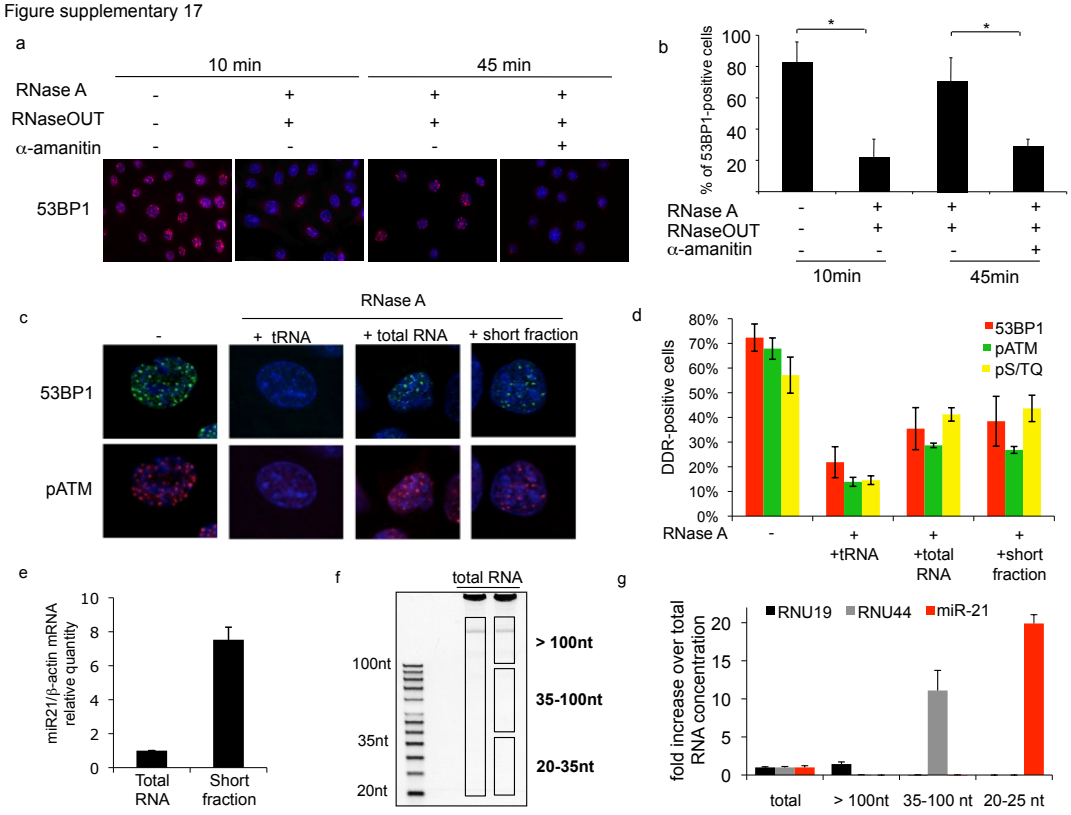

Figure Supplementary 17| α-amanitin inhibits spontaneous DDR foci reformation following RNase A treatment and RNase A inhibition by RNase OUT and incubation with 20-35nt long RNAs is sufficient to restore DDR foci. a. HeLa cells were irradiated and incubated with PBS (-) or RNase A (+). Afterwards, cells were incubated with the RNase A inhibitor RNaseOUT, with or without α-amanitin for 10 or 45 minutes. **b**. Histogram shows the percentage of cells positive for 53BP1 foci. Incubation with α-amanitin prevents 53BP1-foci reformation. Error bars indicate s.e.m. (n=3). Differences are statistically significant (*p-value<0.01). **c**. Irradiation-induced 53BP1 and pATM foci are restored in RNase A and α-amanitin-treated cells upon incubation with 200ng of total RNA or a proportional volume of short RNA-enriched (<200nt) fraction. tRNA (200ng) was used as control. **d.** Histograms show the percentage of cells positive for 53BP1, pATM and pS/TQ foci. Error bars indicate s.e.m. For the quantification shown more than 200 cells from two independent experiments were analysed. **e**. Relative enrichment of miR-21 RNA compared to β-actin mRNA quantity evaluated by qRT-PCR in total RNA and short RNA-enriched fractions. **f.** Total RNA was separated by polyacrylamide gel electrophoresis and gel-extracted. 100, 50 or 20ng of gel extracted total RNA and 50ng of RNA extracted from each gel fraction (>100nt, 35-100nt and 20-35nt) were used for DDR foci reconstitution in HeLa cells. **b.** QRT-PCR analysis of RNU19 (200 nt), RNU44 (61 nt) and miR-21 (22 nt) in the indicated RNA fractions extracted from gel. The enrichment was evaluated as the ratio between PCR cycles (ct values) of the small RNAs analyzed and ct values of β-actin mRNA in each fraction, after normalization over the total RNA fraction. Error bars indicate s.d.

Figure supplementary 18

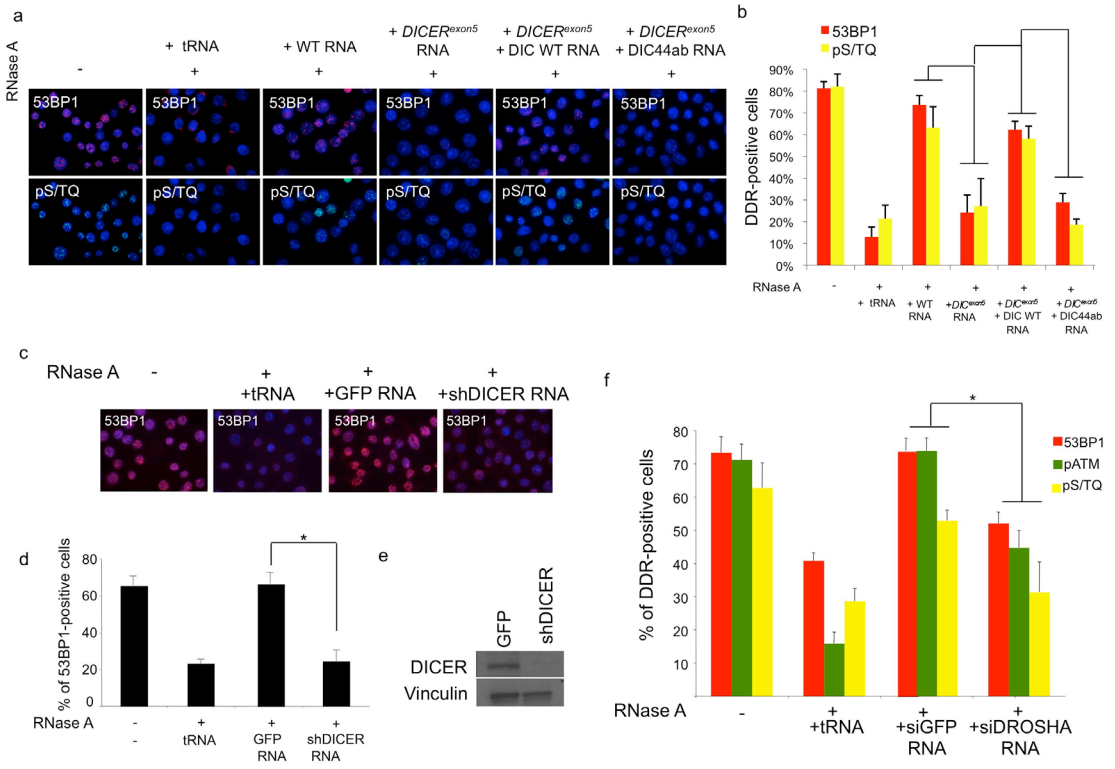

Figure Supplementary 18| DICER and DROSHA RNA products are required for DDR foci reformation. a. Irradiated cells were RNase A-treated and incubated with RNA extracted from the indicated cells. RNA from wild-type cells (WT RNA) or from *DICER*^{exon5} cells transfected with WT DICER (*DICER*^{exon5} +DIC WT RNA) allows 53BP1 foci reformation, while RNA from mock transfected *DICER*^{exon5} cells (*DICER*^{exon5} RNA) or from the same cells transfected with mutant DICER (*DICER*^{exon5} + DIC 44ab RNA) does not. **b.** Histograms show the percentage of cells positive for the indicated DDR markers. Error bars indicate s.e.m. For the quantification shown more than 100 cells were analyzed. **c**. RNA extracted from shDICER- or GFP-transfected cells does not restore irradiation-induced 53BP1 foci in RNase A-treated HeLa cells. tRNA is used as negative control. **d**. Histogram shows the percentage of cells positive for 53BP1 foci. For the quantification shown more than 400 cells from two independent experiments were analysed. **e**. Immunoblotting shows DICER knockdown efficiency**. f.** Histograms show the percentage of cells positive for 53BP1, pATM and pS/TQ foci in irradiated HeLa cells after RNase A treatment and incubation with RNA purified from siGFP and siDROSHA transfected cells. tRNA was used as control. For the quantification shown around 200 cells from two independent experiments were analysed.

Figure supplementary 19

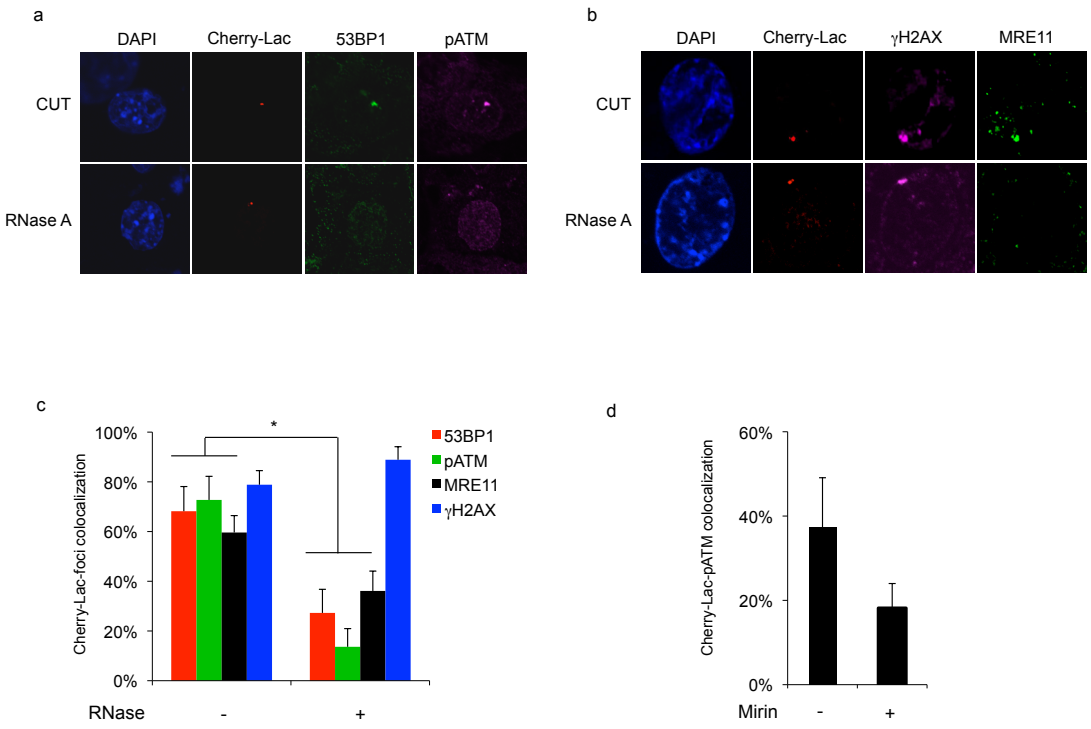

Figure Supplementary 19| pATM and MRE11 focus in cut NIH2/4 cells is sensitive to RNase treatment. a. 53BP1 and pATM foci are lost in RNase A treated cut NIH2/4 cells. **b**. MRE11 foci, but not γH2AX foci, are lost in RNase A treated cut NIH2/4 cells. Error bars indicate s.e.m. (n=3). Differences are statistically significant (*p-$value$<0.05). **c**. Histograms show the percentage of cells in which 53BP1, pATM, MRE11 or γH2AX foci co-localize with the Cherry-Lac focus. **d**. Mirin (100μM) impairs pATM activation on the I-Sce I-induced DSB. Histogram shows the percentage of cells in which pATM focus colocalize with the Cherry-Lac focus. For the quantification shown around 50 cells from two independent experiments were analysed.

Figure supplementary 20

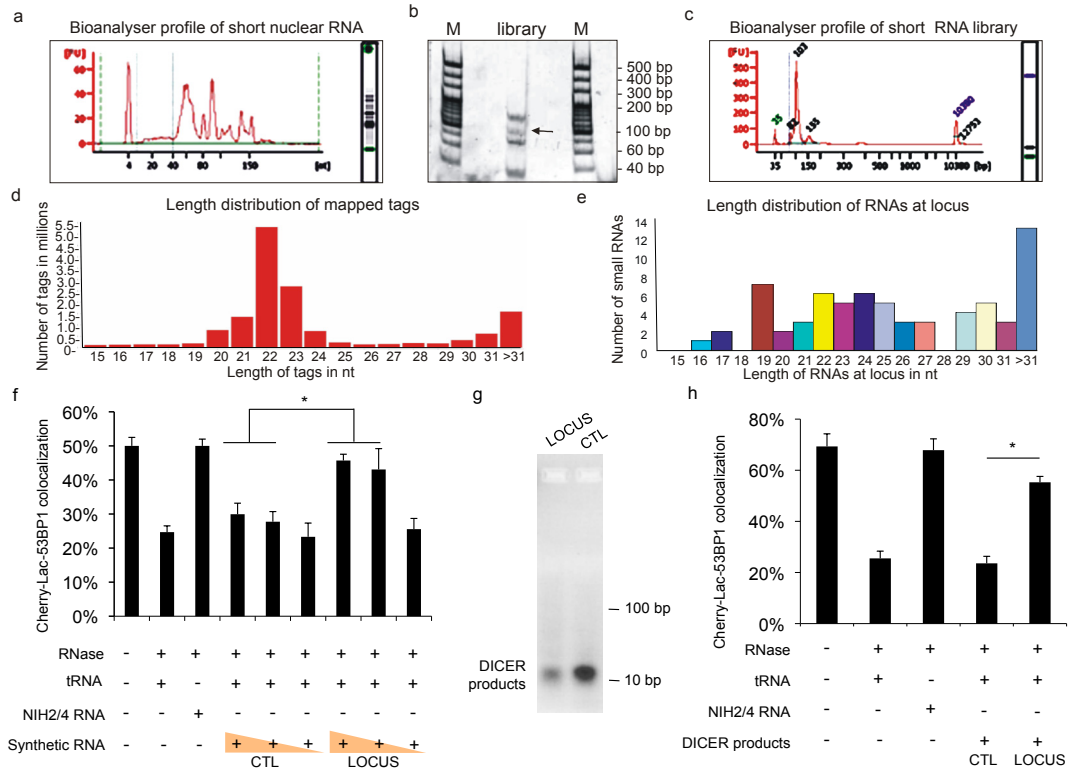

Figure Supplementary 20| Identification of biologically active, locus-specific RNAs. Chemically synthesized locus-specific RNAs and in vitro generated DICER RNA products are sufficient to restore DDR focus formation in RNase A-treated cells. a. Nuclear RNAs shorter than 200 nt were purified and analyzed on the small RNA Bioanalyser kit (Agilent). **b.** Short RNA library was prepared and extracted from 6% polyacrylamide gel (indicated by an arrow at 100 bp). **c.** The integrity of the prepared library was checked using the Agilent DNA high sensitivity kit before sequencing on Illumina GAIIx. **d.** Length distribution of tags in the library. **e.** Length distribution of tags in the library mapping to the exogenous integrated locus combining tags from cut and uncut samples. **f.** A pool of chemically synthesized oligonucleotides mapping to the exogenous locus was tested to restore DDR focus formation in RNase A-treated NIH2/4 cells. Mixed with a constant amount of tRNA, a wide range of concentrations (0.1ng/μl, 0.1pg/μl and 1fg/μl) of locus-specific or control (GFP) RNAs, was used. Site-specific synthetic RNAs, but not control RNAs, induce site-specific DDR activation (up to the concentration of 0.1pg/μl). Histogram shows the percentage of cells in which 53BP1 focus co-localize with the Cherry-Lac focus. Error bars indicate s.e.m. (n=3). Differences are statistically significant (*p-value<0.05). **g**. DICER processing was evaluated by running DICER RNA-products on a 3% agarose gel. **h**. Small double-stranded RNAs generated by recombinant DICER, were tested to restore DDR focus formation in RNase A-treated NIH2/4 cells. 1ng/μl RNA was tested mixed with 800ng of tRNA. Locus-specific DICER RNA products, but not control ones, allow site-specific DDR activation. Histogram shows the percentage of cells in which 53BP1 focus co-localize with the Cherry-Lac focus. Error bars indicate s.e.m. (n=3). Differences are statistically significant (*p-value<0.05).

Figure supplementary 21

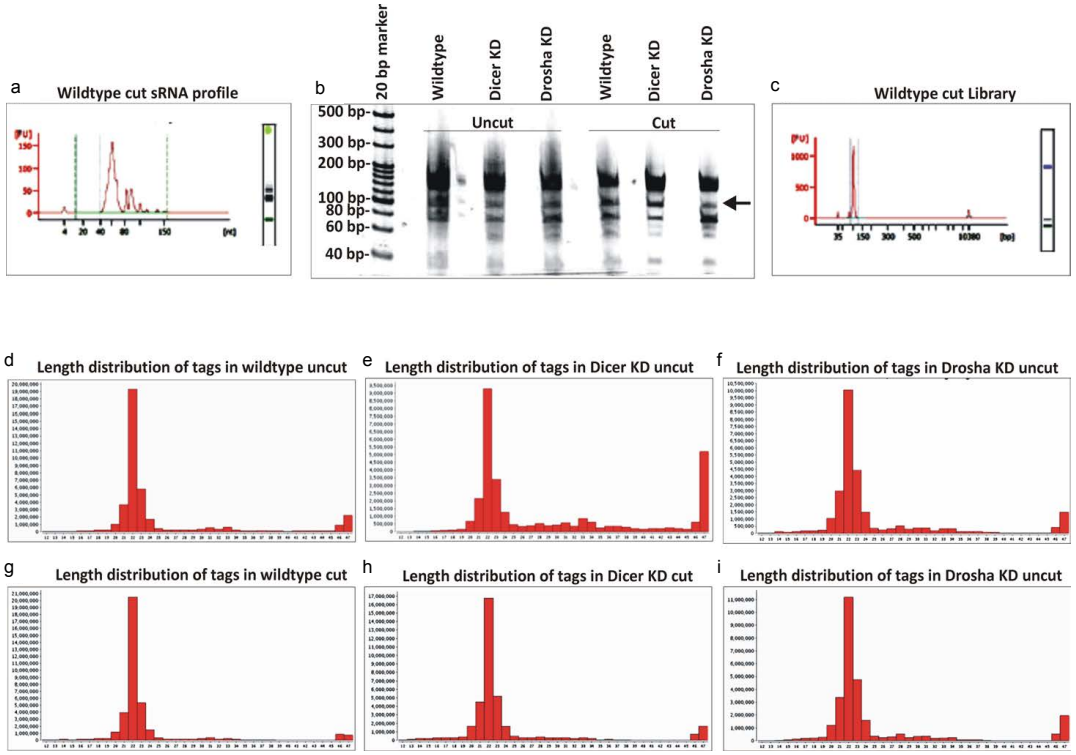

Figure Supplementary 21| Library profile and length distribution of sequenced samples. a. Bioanalyser profile of <200 nt RNAs from wild-type cut sample. **b.** Short RNA libraries were prepared from 40 ng RNA from each sample and run on a 6% PAGE gel. Arrow shows the 100 bp library band of interest. **c.** Wild-type cut library profile. Gel extracted libraries were run on Bioanalyser high sensitivity kit. Sequencing was performed on Hi seq Version 3. **d-i**. Tag length distribution of each library.

Figure supplementary 22

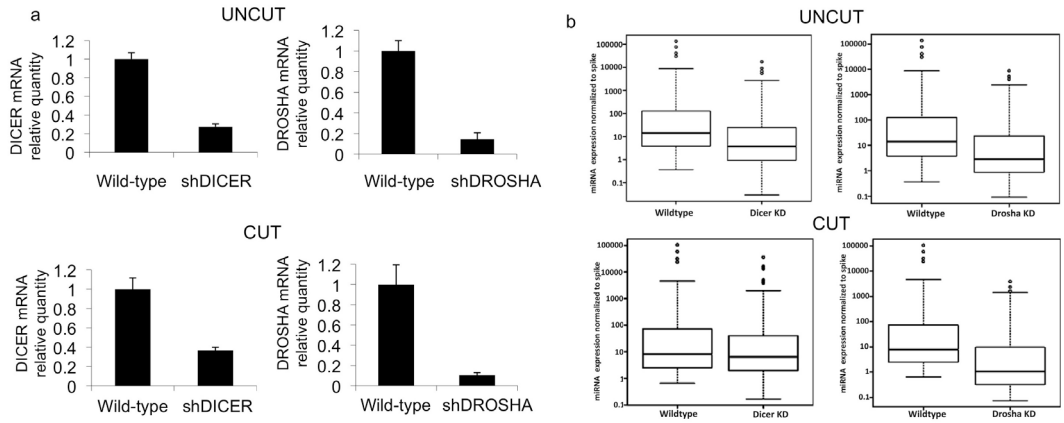

Figure Supplementary 22| DICER and DROSHA knockdown down-regulates miRNAs. a. DICER and DROSHA knockdown by shRNA in uncut and cut samples was evaluated by qRT-PCR. **b.** Reads mapping to the miRNA database miRBase release 18 were normalized with the number of reads of spike in each library. Normalized miRNAs in DICER and DROSHA knockdown samples were compared with wild-type samples before and after cut (as labeled). Statistical significance was calculated using the Wilcoxon signed-rank test. We find that miRNAs are significantly reduced in the DICER and DROSHA knockdown sample compared to the wild-type sample in both cut and uncut conditions (DICER knockdown uncut vs wild-type uncut p =1.544e-263; DROSHA knockdown uncut vs wild-type uncut p =3.843e-279; DICER knockdown cut vs wild-type cut p = 8.911e-84; DROSHA knockdown cut vs wild-type cut p = 1.172e-275).

Figure supplementary 23

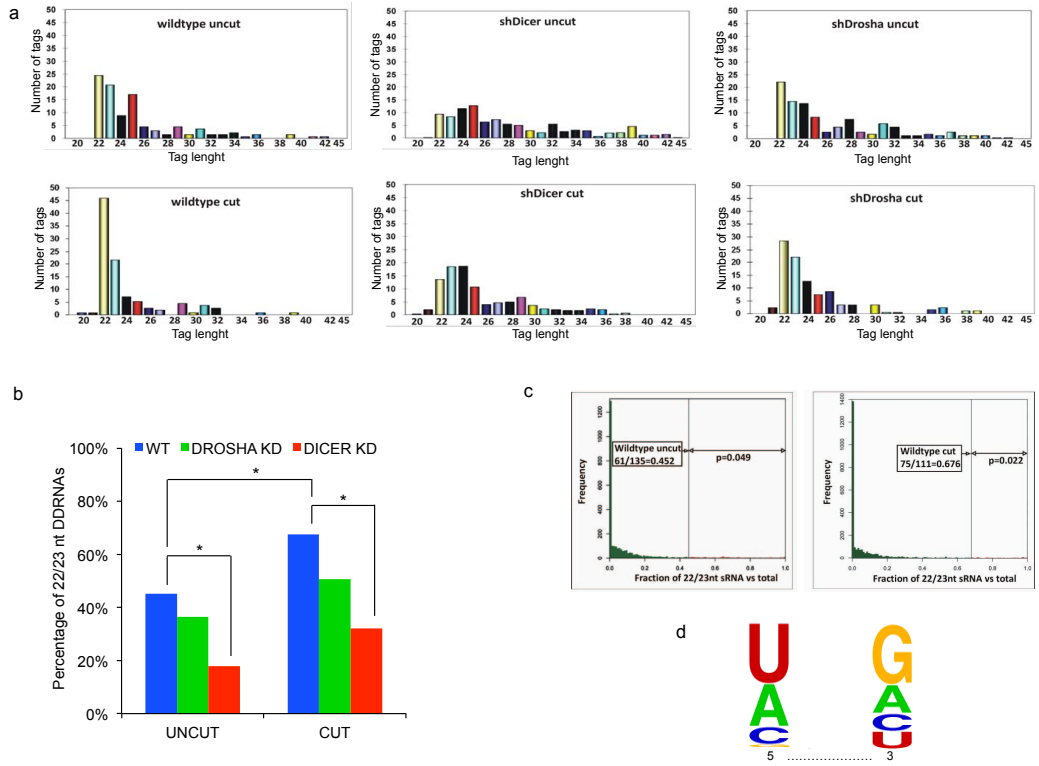

Figure Supplementary 23| Features of short RNAs arising from the locus. a. Length of tags arising from the locus before and after cut. X-axis shows tag lengths in nucleotides and Y-axis depicts number of tags mapping to the locus. The bulk of small RNAs in wild-type samples before and after cut are in the 22-23 nt size range. Among knockdown samples, DICER knockdown shows a broader tag length distribution. **b.** The fraction of 22-23 nt vs total small RNAs at the locus decreases in DICER and DROSHA knockdown samples both in UNCUT and CUT conditions. In DICER knockdown samples, the decrease is statistically significant (in the UNCUT samples p = 4.8e-7, in the CUT samples p=0.029). The fraction of 22-23 nt vs total small RNAs at the locus increases in the wild-type upon cutting (p=0.02). The statistical significance was calculated by fitting a negative binomial model to the small RNA count data and performing a likelihood ratio test, keeping the fraction of 22-23 nt vs total RNAs at the locus fixed across conditions under the null hypothesis and allowing it to vary between conditions under the alternative hypothesis. **c.** The fraction of 22-23 nt reads at the locus is significantly higher than at non miRNA genomic loci. Fractions of 22-23 nt vs total small RNAs at non miRNA genomic loci with at least 50 reads are shown in histograms with the vertical axis depicting their frequency. In each sample, the vertical line depicts the ratio of 22-23 nt RNAs to the total at the locus. The p-value was calculated by summing the area (indicated in red) to the right of this line. We find that the fraction of 22-23 nt vs total small RNAs at the locus studied is significantly higher than the fraction of 22-23 nt tags at non miRNA genomic loci in both uncut (p = 0.049) and cut (p = 0.022) conditions. **d.** The distribution of nucleotides at the 5' and the 3' end of RNA sequences from the locus is significantly different from both the genomic background nucleotide

distribution (p=0.012 at the 5' end and 0.008 at the 3' end) as well as the background nucleotide distribution at the locus (p=0.014 at the 5' end and 1.2e-6 at the 3' end). Specifically, 82.9% sequences start with an A/U and 48.6% sequences end with a G.

Discussion

Here we show that different sources of DNA damage, including oncogenic stress, ionizing irradiation and endonucleases engage the DDR in a manner dependent on DICER and DROSHA RNA products. These DDR-regulating RNAs (DDRNAs) control DDR-foci formation and maintenance, checkpoint enforcement and cellular senescence. This occurs both in cultured human and mouse cells and in different tissues in living zebrafish larvae.

Oncogene activation can trigger DDR and DDR-induced cellular senescence acts as tumor suppressive mechanism[11,42]. DICER inactivation enhances tumor development in a K-Ras-induced mouse model of lung cancer[43] and inactivation of various components of DICER and DROSHA complexes stimulate cell transformation and tumorigenesis[43,44]. More recently, mutations of DICER and TARBP2, a DICER cofactor affecting its stability, have been described in human carcinomas[45,46,47,48,49]. However, individual microRNAs have been reported both to promote and to reduce cell proliferation by regulating stability and translation of mRNAs encoding proteins with different roles in cell proliferation[40]: it is therefore presently unclear how RNAi apparatus inactivation favors tumorigenesis. In the light of our novel findings pointing to a role of DDRNAs in DDR control, a known tumor suppressive mechanism[42], it is tempting to suggest that, in addition to their well-characterized functions in the modulation of gene expression, DICER and DROSHA RNA products may curb cancerous cell proliferation by sustaining DDR activation and this generates the selective pressure for the inactivation of factors involved in their biogenesis.

Genetic ablation of DICER in primary cells has been reported to cause premature senescence[50]. In line with our results, we propose that complete DICER inactivation may dramatically impair the cellular response to DNA damage resulting in massive

DNA-damage accumulation incompatible with proliferation while partial DICER inactivation may weaken DDR enforcement and thus favor genomic instability and tumor progression. This model fits nicely with the recent observations that DICER haploinsufficiency, but not its homozygous deletion, is frequent in human cancer, and that in mice DICER haploinsufficiency promotes cancer, while complete loss of DICER is lethal[44].

We also report that in an *in vitro* cellular system, DDR foci are lost in irradiated cells following RNase A treatment and that site-specific DDRNAs, even if generated by chemical synthesis or upon *in vitro* cleavage by recombinant DICER, are sufficient to restore them. This suggests that DDRNAs are locally generated and favor the assembly of DDR factors in the shape of detectable DDR foci. Indeed RNA sequencing confirmed the presence of small RNAs arising from the integrated exogenous locus which are induced upon cut. Comparison with small RNAs generated at other non-miRNA genomic loci indicates that they are distinct from products of RNA degradation and their nucleotide bias at 5' end and 3' end indicates that these RNAs are processed at preferential RNA precursors sites.

Although at present how DDRNAs act to control DDR activation has not been elucidated in full, the observation that they act in a manner dependent on the MRN complex suggests they act as upstream elements of the canonical DDR signaling cascade. Interestingly, short MRN-dependent DNA oligonucleotides have been shown to stimulate ATM activity[51]. Although it may be conceived that DDRNAs act by base-pairing to nascent RNA at the DNA damage site, their demonstrated biological activity following RNase A treatment and in the presence of a-amanitin makes this possibility unlikely.

Although novel and unanticipated, our results are consistent with the emerging

evidence supporting a role for RNA molecules in DDR. Indeed, an epistasis map generated in fission yeast has recently shown that DDR components display genetic interactions with the RNAi machinery[52] and components of the large DROSHA complex have been identified in a ATM-dependent phosphoproteome screen[53]. In *Drosophila*, repeated DNA integrity is dependent on RNAi pathway[54]. In *Saccharomyces cerevisiae* and in *Oxytricha Trifallax* RNA orchestrates recombination and RNA can function as a template for DNA repair events in *S. cerevisiae*[55,56,57]. It is also intriguing to observe that like several DDR factors, which are inactivated early in apoptosis in order to prevent DDR activation[58], also DICER is specifically cleaved by caspases during apoptosis[59]. Recently, ATM has been shown to directly modulate the biogenesis of DICER and DROSHA RNA products by phosphorylating KSRP[60]. Furthermore, several other DDR factors such as 53BP1, BRCA1, KU and ATR have been previously reported to bind to RNA[61,21,62,63]. Moreover, while this manuscript was under evaluation, the presence of DICER-dependent RNAs at DSB was reported[64]. The observed dependency on DICER and DROSHA suggests that DDRNAs may also rise from cleavage of folded RNA.

Finally, it is worth noticing that the here-described novel functions of DICER and DROSHA, components of the RNAi machinery, in the modulation of DDR are consistent with the well-established and evolutionary-conserved role of this apparatus in preserving genome integrity from viral invaders, transposons and retroelements[65,36].

References

31 Guttman, M. *et al.* Chromatin signature reveals over a thousand highly conserved large non-coding RNAs in mammals. *Nature* **458**, 223-227, doi:10.1038/nature07672 (2009).

32 Drinnenberg, I. A. *et al.* RNAi in budding yeast. *Science* **326**, 544-550, doi:10.1126/science.1176945 (2009).

33 Clemson, C. M. *et al.* An architectural role for a nuclear noncoding RNA: NEAT1 RNA is essential for the structure of paraspeckles. *Mol Cell* **33**, 717-726, doi:10.1016/j.molcel.2009.01.026 (2009).

34 Wutz, A. RNAs templating chromatin structure for dosage compensation in animals. *Bioessays* **25**, 434-442 (2003).

35 Orom, U. A. *et al.* Long noncoding RNAs with enhancer-like function in human cells. *Cell* **143**, 46-58, doi:10.1016/j.cell.2010.09.001 (2010).

36 Berezikov, E. Evolution of microRNA diversity and regulation in animals. *Nature reviews. Genetics* **12**, 846-860, doi:10.1038/nrg3079 (2011).

37 Farazi, T. A., Juranek, S. A. & Tuschl, T. The growing catalog of small RNAs and their association with distinct Argonaute/Piwi family members. *Development* **135**, 1201-1214, doi:10.1242/dev.005629 (2008).

38 Lee, H. C. *et al.* qiRNA is a new type of small interfering RNA induced by DNA damage. *Nature* **459**, 274-277, doi:10.1038/nature08041 (2009).

39 Ding, L. & Han, M. GW182 family proteins are crucial for microRNA-mediated gene silencing. *Trends in cell biology* **17**, 411-416, doi:10.1016/j.tcb.2007.06.003 (2007).

40 Esquela-Kerscher, A. & Slack, F. J. Oncomirs - microRNAs with a role in cancer. *Nat Rev Cancer* **6**, 259-269 (2006).

41 He, L., He, X., Lowe, S. W. & Hannon, G. J. microRNAs join the p53 network--another piece in the tumour-suppression puzzle. *Nat Rev Cancer* **7**, 819-822, doi:10.1038/nrc2232 (2007).

42 Halazonetis, T. D., Gorgoulis, V. G. & Bartek, J. An oncogene-induced DNA damage model for cancer development. *Science* **319**, 1352-1355, doi:10.1126/science.1140735 (2008).

43 Kumar, M. S., Lu, J., Mercer, K. L., Golub, T. R. & Jacks, T. Impaired microRNA processing enhances cellular transformation and tumorigenesis. *Nat Genet* **39**, 673-677, doi:10.1038/ng2003 (2007).

44 Kumar, M. S. *et al.* Dicer1 functions as a haploinsufficient tumor suppressor. *Genes Dev*, doi:10.1101/gad.1848209 (2009).

45 Merritt, W. M. *et al.* Dicer, Drosha, and outcomes in patients with ovarian cancer. *The New England journal of medicine* **359**, 2641-2650, doi:10.1056/NEJMoa0803785 (2008).

46 Hill, D. A. *et al.* DICER1 mutations in familial pleuropulmonary blastoma. *Science* **325**, 965, doi:10.1126/science.1174334 (2009).

47 Melo, S. A. *et al.* A TARBP2 mutation in human cancer impairs microRNA processing and DICER1 function. *Nat Genet* **41**, 365-370, doi:10.1038/ng.317 (2009).

48 Torres, A. *et al.* Major regulators of microRNAs biogenesis Dicer and Drosha are down-regulated in endometrial cancer. *Tumour biology : the journal of the International Society for Oncodevelopmental Biology and Medicine* **32**, 769-776, doi:10.1007/s13277-011-0179-0 (2011).

49 Heravi-Moussavi, A. *et al.* Recurrent somatic DICER1 mutations in nonepithelial ovarian cancers. *The New England journal of medicine* **366**, 234-242, doi:10.1056/NEJMoa1102903 (2012).

50 Mudhasani, R. *et al.* Loss of miRNA biogenesis induces p19Arf-p53 signaling and senescence in primary cells. *J Cell Biol* **181**, 1055-1063, doi:10.1083/jcb.200802105 (2008).

51 Jazayeri, A., Balestrini, A., Garner, E., Haber, J. E. & Costanzo, V. Mre11-Rad50-Nbs1-dependent processing of DNA breaks generates oligonucleotides that stimulate ATM activity. *The EMBO journal* **27**, 1953-1962, doi:10.1038/emboj.2008.128 (2008).

52 Roguev, A. *et al.* Conservation and rewiring of functional modules revealed by an epistasis map in fission yeast. *Science* **322**, 405-410, doi:10.1126/science.1162609 (2008).

53 Bensimon, A. *et al.* ATM-Dependent and -Independent Dynamics of the Nuclear Phosphoproteome After DNA Damage. *Sci Signal* **3**, rs3, doi:10.1126/scisignal.2001034 (2010).

54 Peng, J. C. & Karpen, G. H. H3K9 methylation and RNA interference regulate nucleolar organization and repeated DNA stability. *Nat Cell Biol* **9**, 25-35, doi:10.1038/ncb1514 (2007).

55 Derr, L. K. & Strathern, J. N. A role for reverse transcripts in gene conversion. *Nature* **361**, 170-173, doi:10.1038/361170a0 (1993).

56 Nowacki, M. *et al.* RNA-mediated epigenetic programming of a genome-rearrangement pathway. *Nature* **451**, 153-158 (2008).

57 Storici, F., Bebenek, K., Kunkel, T. A., Gordenin, D. A. & Resnick, M. A. RNA-templated DNA repair. *Nature* **447**, 338-341, doi:10.1038/nature05720 (2007).

58 Smith, G. C., d'Adda di Fagagna, F., Lakin, N. D. & Jackson, S. P. Cleavage and inactivation of ATM during apoptosis. *Mol Cell Biol* **19**, 6076-6084. (1999).

59 Ghodgaonkar, M. M. *et al.* Abrogation of DNA vector-based RNAi during apoptosis in mammalian cells due to caspase-mediated cleavage and inactivation of Dicer-1. *Cell Death Differ* **16**, 858-868, doi:10.1038/cdd.2009.15 (2009).

60 Zhang, X., Wan, G., Berger, F. G., He, X. & Lu, X. The ATM kinase induces microRNA biogenesis in the DNA damage response. *Molecular cell* **41**, 371-383, doi:10.1016/j.molcel.2011.01.020 (2011).

61 Yoo, S. & Dynan, W. S. Characterization of the RNA binding properties of Ku protein. *Biochemistry* **37**, 1336-1343, doi:10.1021/bi972100w (1998).

62 Ganesan, S. *et al.* BRCA1 supports XIST RNA concentration on the inactive X chromosome. *Cell* **111**, 393-405. (2002).

63 Kedde, M. *et al.* Telomerase-independent regulation of ATR by human telomerase RNA. *J Biol Chem* **281**, 40503-40514, doi:10.1074/jbc.M607676200 (2006).

64 Wei, W. *et al.* A Role for Small RNAs in DNA Double-Strand Break Repair. *Cell* **149**, 101-112, doi:10.1016/j.cell.2012.03.002 (2012).

65 Hannon, G. J. RNA interference. *Nature* **418**, 244-251, doi:10.1038/418244a (2002).